Tectonophysics 578 (2012) 87–97

Contents lists available at SciVerse ScienceDirect

Tectonophysics

journal homepage: www.elsevier.com/locate/tecto

Estimation of rupture processes of the 2008 Wenchuan Earthquake from joint analyses of two regional seismic arrays

Bor-Shouh Huang [a,*], Jiu-Hui Chen [b], Qi-Yuan Liu [b], Yue-Gau Chen [c], Xi-Wei Xu [b], Chun-Yong Wang [d], Shiann-Jong Lee [a], Zhen-Xing Yao [e]

[a] Institute of Earth Sciences, Academia Sinica, Taipei
[b] State Key Laboratory of Earthquake Dynamics, Institute of Geology, China Earthquake Administration, Bejing
[c] Department of Geosciences, National Taiwan University, Taipei
[d] Institute of Geophysics, China Earthquake Administration, Beijing
[e] Institute of Geology and Geophysics, Chinese Academy of Sciences, Beijing

ARTICLE INFO

Article history:
Received 25 November 2010
Received in revised form 17 November 2011
Accepted 19 December 2011
Available online 29 December 2011

Keywords:
Rupture processes
Source image
Seismic array
Back-projection

ABSTRACT

We estimated the source rupture of the 2008 Wenchuan Earthquake (Ms 8), China, based on a back-projection of seismic waves to their source plane, using data from regional broadband arrays in Taiwan and northern Vietnam. Observations from these arrays, located at different azimuths, were processed to evaluate the spatio-temporal rupture behavior of the fault. The seismic energy spot converted from windowed array waveforms was back-projected to the rupture plane of the earthquake, to image the instantaneous slip on the fault plane. Rupture processes were reconstructed based on the imaged time-dependent seismic energy radiating from the earthquake fault plane. The high station density of both arrays enabled a detailed examination of the rupture processes. The results indicate that the 2008 Wenchuan Earthquake had a rupture duration of approximately 100 s, with major asperities radiating energy at 50 s after the initiation of rupture. The location of asperities is in good agreement with sections of the earthquake fault along which major damage occurred, such as along the Yingxiu–Beichuan Fault. The radiated seismic energy shows a complex spatial distribution on the fault plane. Our analysis indicates that the rupture initiated at the epicenter and extended to the northeast for approximately 280 km. The average rupture velocity of this earthquake was approximately 2.8 km/s.

1. Introduction

The Ms 8 Wenchuan earthquake occurred on 12 May 2008 near the western edge of the Sichuan Basin in China (Fig. 1). According to results reported by the U.S. Geological Survey (USGS), the magnitude of the earthquake was Mw 7.9 or Ms 8.0, at a depth of 19 km at 30.986°N, 103.364°E. Of note, this earthquake produced fault ruptures over a distance of 270 km (Burchfiel et al., 2008). The earthquake induced numerous landslides and caused severe damage over a wide area, resulting in 69,195 fatalities, 18,392 missing (due mainly to landslides), and 374,177 injured (National Earthquake Information Center, USGS). Over 5 million people were left homeless and 46 million people were significantly impacted by the earthquake; 21 million buildings were damaged and the total monetary cost was estimated to be over 845 billion Chinese Yuan.

The Wenchuan earthquake occurred on the Longmenshan Fault, which is a NE–SW-striking thrust fault. Tectonic stresses within the Longmenshan fault zone result from the eastward movement of crust of the high Tibetan Plateau, against the strong and stable crustal block that underlies the Sichuan Basin and southeastern China (Zhang et al., 2010). The Longmenshan fault zone contains three major faults: the front ridge fault (or the Guanxian–Anxian Fault), the central fault (Yingxiu–Beichuan Fault), and the behind ridge fault (Wenchuan–Maowen Fault). Along strike, the fault zone can be roughly divided into three first-order segments: southern (or southwestern), middle, and northern (or northeastern). The Wenchuan earthquake created surface ruptures along the middle and northern segments of the Yingxiu–Beichuan Fault, and along the southern segment of the Guanxian–Anxian Fault (Xu et al., 2009a, 2009b).

The Wenchuan earthquake has been analyzed in many studies (e.g., Chen et al., 2009; Huang et al., 2008b), all of which reported the common feature of an almost pure reverse-slip focal mechanism and shallow seismicity. The mapping of surface faults has revealed that the complicated fault structure appears to comprise several faults and may have simultaneously ruptured parallel faults in the southern region (e.g., Dong et al., 2008). The mapped surface displacements range up to approximately 6 m (Xu et al., 2009b). The source mechanism, slip distribution, and geodetic observations indicate that the

* Corresponding author. Tel.: +886 2 27839910.
E-mail address: hwbs@earth.sinica.edu.tw (B.-S. Huang).

0040-1951/$ – see front matter © 2011 Elsevier B.V. All rights reserved.
doi:10.1016/j.tecto.2011.12.026

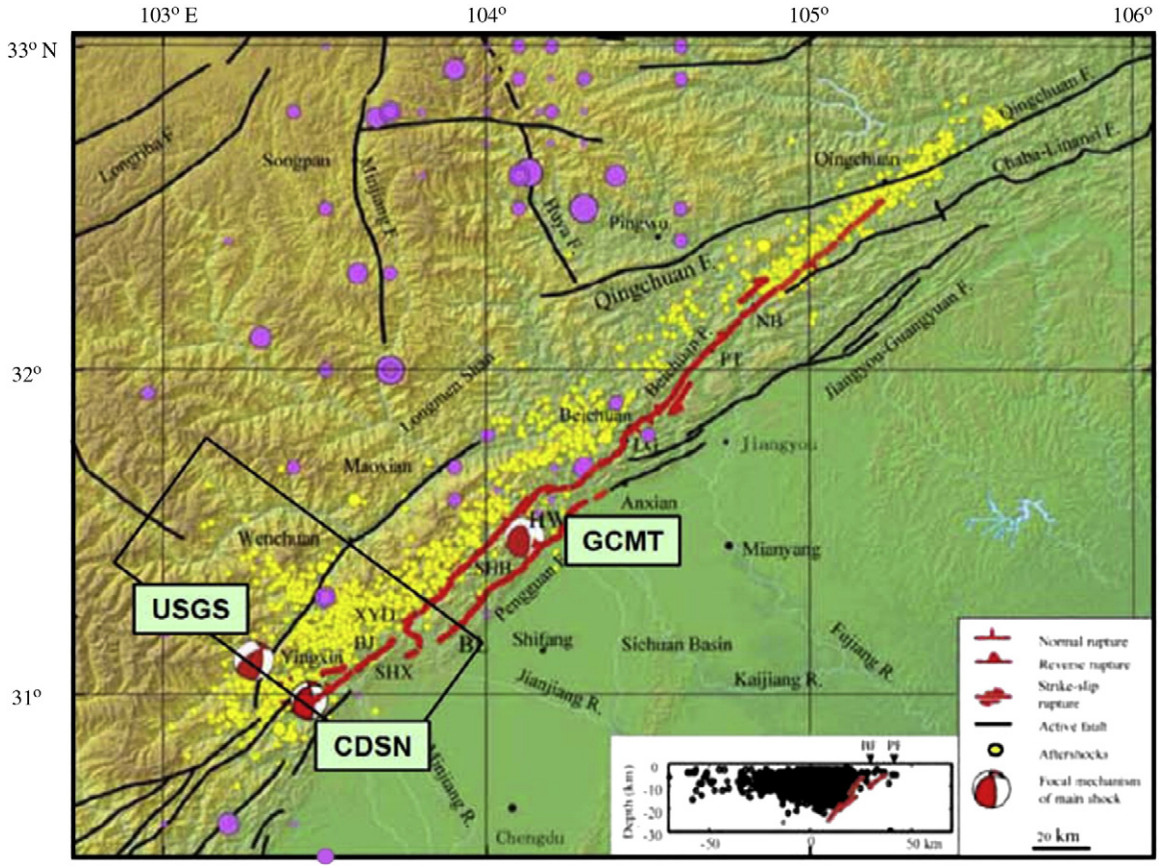

Fig. 1. Simplified topographical map showing the distribution of active faults in the Longmen Shan region and surface ruptures of the 2008 Wenchuan earthquake along the Beichuan and Pengguan faults, Longmenshan thrust belt (modified from Xu et al., 2008). The focal mechanisms of the main shock, as shown on the map, were determined by the United States Geological Survey (USGS), Global CMT Project (GCMT), and the China Digital Seismic Network (CDSN). Historical destructive earthquakes and aftershocks of the 2008 event are shown as pink and yellow circles, respectively. The location of the aftershock cross-section (shown in the inset) is indicated by the black rectangle across the epicentral area.

faults dip to the northwest at an unknown dip angle with significant slip occurring from the surface to depths of 15–20 km.

Previous studies have described the geometry of this earthquake ruptured fault as a curved plane with decreasing dip from the surface to depth (Chen et al., 2009; Shen et al., 2009). According to reports by the International Seismological Centre (ISC), there are no historical records of $M>6.5$ events directly within the Longmenshan, and no events of a comparable size to the 2008 earthquake have been recorded in this region. Furthermore, the northern segment of the Longmenshan fault zone was inactive during the Quaternary (Burchfiel et al., 2008; Zhang et al., 2008). Studies of the 2008 Wenchuan earthquake are expected to enhance our understanding of the status of and relations among the major faults in the region. Such information is important because the rupture behavior of this earthquake is of wide interest.

Numerous studies have estimated the slip distribution for the mainshock of the Wenchuan earthquake using teleseismic waveform inversion (Du et al., 2009; ERI, 2008; Ji, 2008; Nagoya, 2008; Nishimura and Yagi, 2008; Wang et al., 2008). All of these models showed that the earthquake rupture propagated mainly unilaterally from the hypocenter toward the northeast over a distance of more than 220 km, with an area of large slip near the hypocenter or slightly to its northeast. Most of the models also show a general image of a large slip at 100–150 km to the northeast of the hypocenter. For all of these studies, the total moment was in the range of 0.7 to 1.2 10^{21} N–M, which corresponds to Mw 7.8–7.9. These data are important in assessing the future risk of a large earthquake in the region and in mitigating the risk to society.

Seismic arrays can detect and locate earthquakes and seismic structures with a better signal-to-noise ratio than in the case of a single seismic station (Rost and Thomas, 2002). Since the megathrust tsunamigenic M9.1 Sumatra earthquake in 2004 (Ishii et al., 2005; Krüger and Ohrnberger, 2005a), array methods have also been applied to large earthquakes to determine kinematic parameters such as the rupture extent, direction, duration, and velocity (Ishii et al., 2007; Xu et al., 2009c; Zhang and Ge, 2010). However, although most images from teleseismic waveform inversions and array stacking studies show a similar rupture pattern, there are differences in the details (e.g., the high-frequency content) of the slip distribution between the various results. This discrepancy may arise because seismograms are located at more than 30° from the epicenter and are dominated by long periods. It is clear that selected teleseismic waveforms with distances greater than 30° would exclude the waveform complexity induced by upper mantle triplication (Walck, 1984) and would therefore stabilize the inversion results. However, the analysis of less-coherent high-frequency seismic energy may prevent a detailed examination of the source rupture of large events.

In the present study, we sought to image the Wenchuan earthquake source rupture from two regional array observations, using a back-projection approach similar to that described by Ishii et al. (2005) in imaging the complex source rupture process of the 2004 Sumatra–Andaman earthquake. The two arrays employed in this study (i.e., broadband arrays from Taiwan and northern Vietnam) provide similar high-quality regional seismic data to that of the Hi-Net array in Japan (Mori and Smyth, 2009) and are located at critical azimuths in terms of resolving the rupture processes of the Wenchuan earthquake. The centers of the Vietnam and Taiwan arrays are located at approximately 9° and 17° from the epicenter, respectively (Fig. 2). Individual and joint estimations of the rupture processes of this

event were made to enable the interpretation of the detailed rupture processes.

The present results indicate that the rupture initiated at the southern end of the earthquake fault and propagated mainly unilaterally toward the northeast at an average speed of about 2.8 km/s for approximately 280 km. A large asperity was imaged to close a patch at 100–170 km northeast of the epicenter, which relates to high-frequency seismic energy radiating from a segment of the Yingxiu–Beichuan Fault.

2. Methods

The P-wave train of a large earthquake is generated by the spatio-temporal distribution of fault slip, with subsequent radiation of seismic energy from slips on asperities upon the fault plane. The first-arriving energy comes from the hypocenter, whereas later-arriving energy is due to slip at and behind the rupture front. In the present study, we employed an approach similar to that described by Ishii et al. (2005), using data from multiple regional arrays to image the complex source rupture process of the 2008 Wenchuan Earthquake.

In principle, our analysis applies back-projection mapping, in which seismograms are stacked for each possible source location to obtain a direct image of the source (Huang, 2001; Huang, 2008; Huang et al., 2004, 2008a). The stacking procedure sums the energy radiated from the given source points constructively, and cancels out all other energy present in the array seismograms. The stacked images are formed as follows:

$$S(x,t) = \frac{1}{N}\sum_{k=1}^{N} \alpha_k u_k\left(t - t(x)_k^p\right), \tag{1}$$

where α_k is the weighting factor for each seismogram; u_k is the seismogram at the kth station, which is corrected for first arrivals that traveled from the hypocenter predicted by a theoretical model; $t(x)_k^p$ is the predicted travel time between stations k and x; x is the position of the potential source location; and t is time with respect to the onset. $S(x,t)$ can be expressed as a normalized sum over N seismograms, providing an estimate of the relative intensity of P-wave radiation from the rupture zone. To make a joint estimation, $S_i(t)$ from each potential source location x and individual array i are stacked over again for each time step to obtain a combined source image; thus,

$$S(t) = \prod_{i=1}^{M} w_i S_i(t), \tag{2}$$

where M is the number of arrays. Here, w_j are real, normalized, user-defined weights that can be applied to manipulate the relative contribution of each array. The new combined source image, which stacks images approaching from several azimuths, is expected to have a higher spatial resolution than that of a single array, which is an advantage in imaging the source rupture.

3. Data

Data were obtained from two broadband networks (Fig. 2): the Broadband Array in Taiwan for Seismology (BATS) and the Vietnam Broadband Seismic Network (VBSN). BATS is a regional broadband seismic network (Fig. 3) comprising stations of the Institute of Earth Sciences of Academia Sinica (IESAS) and the Central Weather Bureau Seismic Network (CWBSN) (Kao et al., 1998). The network is designed to monitor seismic activity, to determine the regional earthquake source mechanisms in the Taiwan region, and to provide high-quality broadband seismic waveforms for scientific research. All of the IESAS stations are equipped with Streckeisen STS-1 or STS-2 sensors and 24-bit digital recorders (Quanterra Q-330), and all of the CWBSN stations are equipped with Guralp CMG-40TD sensors and CMG-DM24S6 recorders. For all stations, data are sampled at 100 Hz.

For regional events, the integrated BATS seismic network, consisting of 51 instruments throughout Taiwan and surrounding islands at spacing of approximately 40 km, can be considered a dense broadband

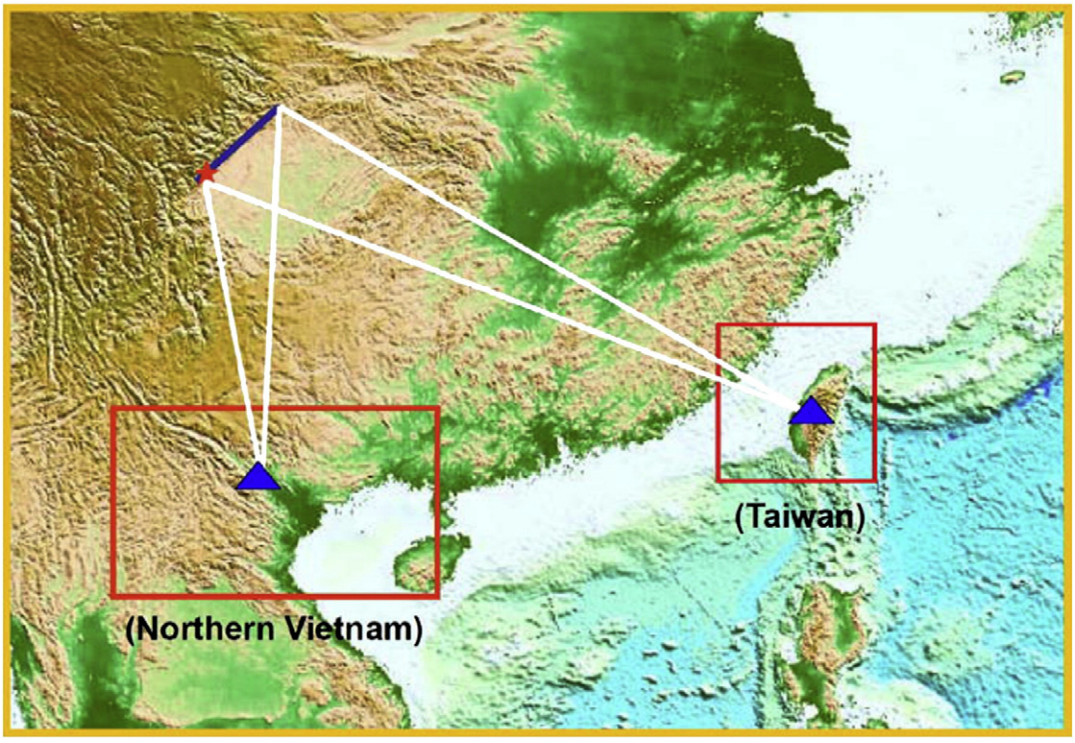

Fig. 2. Regional topographical map showing the location of the earthquake fault (thick blue line) of the 2008 Wenchuan earthquake, and the geometry of two regional seismic arrays used in this study, located in Taiwan and northern Vietnam. The epicenter is indicated by the red star. White lines show the range of paths from the ruptured fault to the array centers (solid blue triangles).

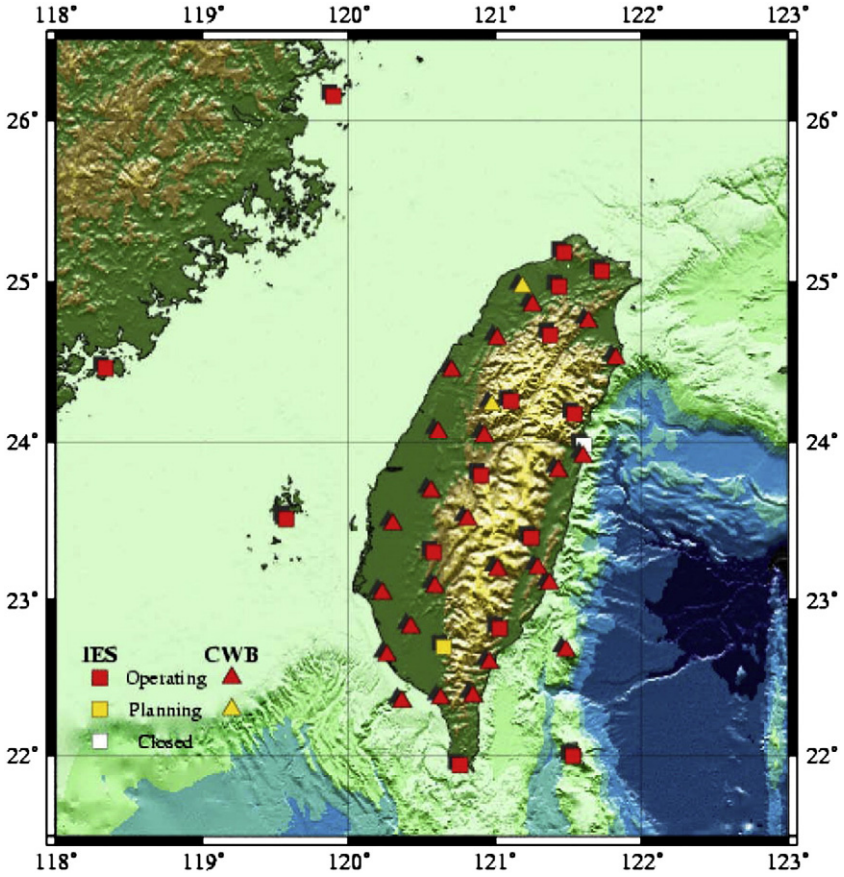

Fig. 3. Distribution of seismic stations in Taiwan and on surrounding islands. For more information, see the BATS Web site (http://bats.earth.sinica.edu.tw/).

seismic array, employed to determine source rupture processes of great earthquakes at regional and teleseismic distances. BATS obtained a continuous recording of the 2008 Wenchuan earthquake sequence. We used 45 of the available BATS stations in the present analysis. These array seismograms have generally similar waveforms, and no stations were included with strong site responses or instrumental problems. The array is located at distances of 16.5°–18.3° from the earthquake and clearly records the direct P-wave. Data were band-pass filtered within 0.2 and 1.0 Hz, and were aligned on the first arrival using waveform cross-correlations.

Fig. 4 shows examples of the P-waves used in the present study. The P-wave onset of this event is remarkably coherent among the

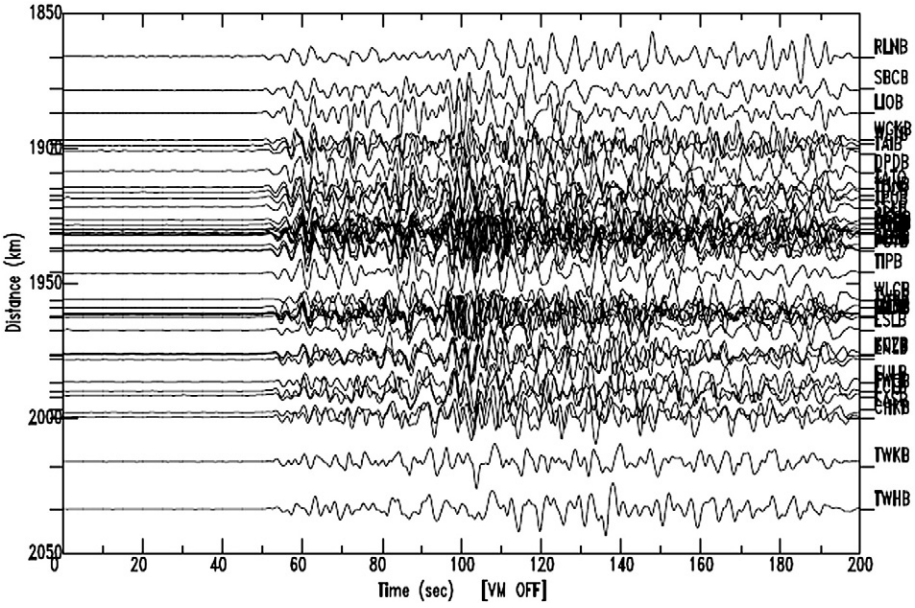

Fig. 4. Aligned vertical-component velocity seismograms of the 2008 Wenchuan earthquake selected from BATS stations. The seismograms were filtered and normalized individually. The vertical axis shows the distance of each station from the epicenter. After removing high-noise traces and some remote array stations, 45 seismograms were used in this study for seismogram stacking.

different stations in the array, but later parts of the P-wave train are complicated by multiple, overlapping arrivals of seismic energy from different portions of the rupture. The duration is 80–90 s, which indicates the general duration of the earthquake source. For BATS stations located to the east of the Wenchuan earthquake, the N–S orientation of the ruptured fault plane resulted in a large azimuth gap between the ruptured fault and the BATS array (nearly 10°), as shown in Fig. 2. However, because of the regional distance from the earthquake fault to seismic array, the BATS seismograms provide sufficient spatial resolution for spatio-temporal imaging of source processes.

VBSN is a portable broadband seismic array (Fig. 5) developed jointly by researchers from Vietnam and Taiwan for imaging and interpreting crust and mantle structures beneath northern Vietnam, including the geodynamic evolution of the Red River Shear Zone (RRSZ), and for testing as an early warning system for earthquakes and tsunamis (Huang et al., 2009). Since 2005, 25 broadband seismic stations have been installed in northern Vietnam to acquire high-density seismic data with a wide dynamic range. Four of the stations employ Streckeisen STS-2 sensors; the rest employ Nanometrics Trillium 40 broadband sensors. The output from the seismometers is recorded on a Quanterra/Kinemetrics Q330 recorder with 24-bit analogue-to-digital conversion. The ground motion signal is recorded continuously and digitized at a rate of 100 samples per second. This array has a uniform spatial distribution in northern Vietnam and covers the RRSZ and the region of high seismic activity in northwestern Vietnam, with an inter-station spacing of approximately 100 km (Fig. 5).

The 2008 Wenchuan earthquake was well recorded by the VBSN array. In the present analysis, we used data from all 22 of the available stations. This array is located at distances of 8.4°–11.5° from the earthquake. The first arrivals of these observations were predicted to be Pn phases by the earth model IASP91 (Kennett and Engdahl, 1991). Fig. 6 shows examples of the VBSN array seismograms used in the present study. The Pn-wave onset of this event is remarkably coherent among the stations in the array. The azimuth gap within the ruptured fault and this array is almost 14°, which is larger than the azimuth gap of the BATS array (Fig. 2). This larger gap arises because of the shorter distances to the epicenter compared with BATS (although VBSN is located southeast of the Wenchuan earthquake and the N–S orientation of the ruptured fault plane). As for BATS, the spatial resolution of seismograms recorded by VBSN is sufficient for spatio-temporal imaging of source processes.

4. Analysis and results

To reconstruct the source rupture on the fault plane, we used a back-projection approach, as described in the Methods section, to image the energy radiated from the source. This approach uses back-projection mapping, in which seismograms are stacked for each possible source location to obtain a direct image of the source. In practice, because the P-wave travel times provide a poor constraint on the source depth, to determine the stacked image we only back-projected to source locations as a function of latitude and longitude at the hypocenter depth. For back-projection calculations of the Wenchuan earthquake, we set a grid of 200×10 points (400×20 km) in the source area, covering the aftershock region. The travel time from each station to any possible source was computed using a 1D velocity model (IASP91).

We checked the different branches of seismic energy that arrived at BATS stations from the source area, using major aftershocks of the Wenchuan earthquake, and observed no clear multiple P-wave arrivals. We identified the branch of major seismic energy and employed it for future array stacking, and back-projected all seismograms recorded by BATS stations (Fig. 4) according to the identified P phase. The initial arrival of the first time window was assumed to originate from the grid point corresponding to the earthquake hypocenter. Relative time shifts for each time series were calculated using the theoretical travel times from the station to the grid point, using the IASPEI91 model. We constructed a data volume of snapshots of source grid points at various time steps, and obtained images over the 100-second duration of the rupture. The BATS seismograms generally highlight a rupture zone consistent with the epicenter during the early stages of the initiation of the source rupture (Fig. 7). After a short period of remaining stationary, the rupture zone began to move continuously northeastward away from the epicenter for approximately 80 s. Our analysis enabled the reconstruction of source images and their spatial locations (see Fig. 7). These images can be used to determine the nature of rupture behavior. This method

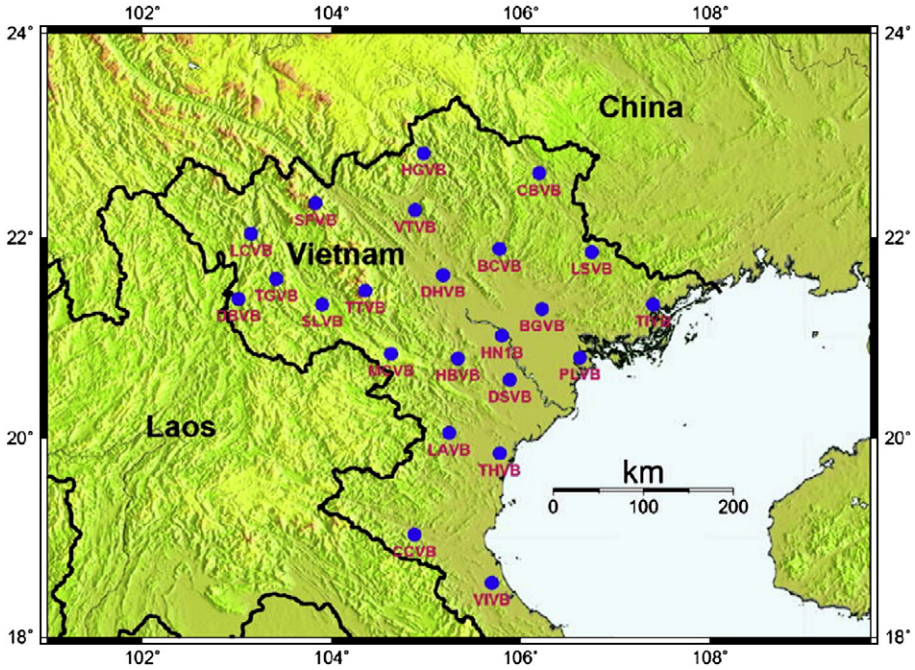

Fig. 5. Distribution of seismic stations (blue circles) in northern Vietnam. Station codes are written in red.

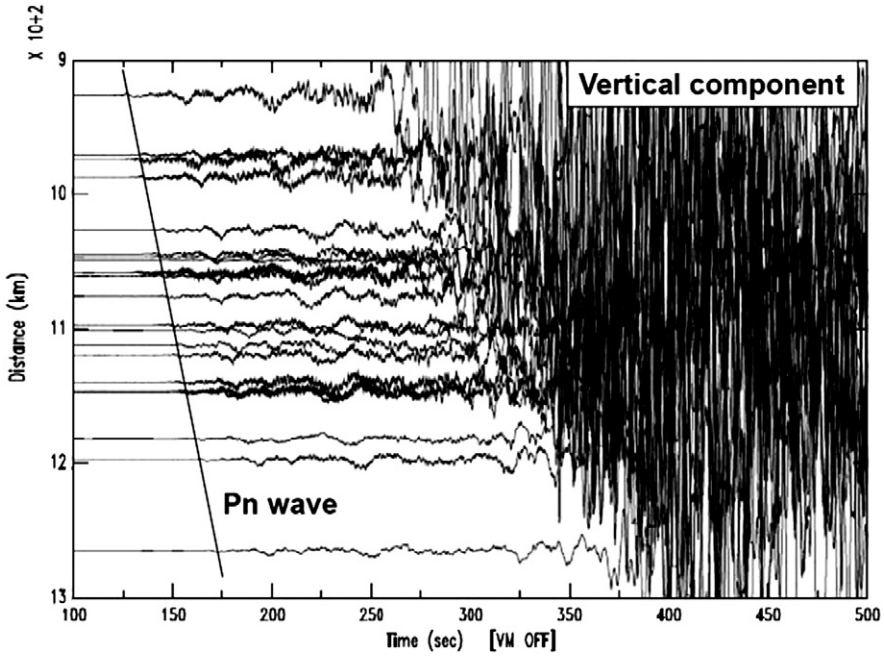

Fig. 6. Distance–traveltime diagram for vertical-component velocity seismograms of the 2008 Wenchuan earthquake selected from VBSN stations. The seismograms were normalized individually. The horizontal axis indicates the time from the earthquake origin, and the vertical axis shows the distance of each station from the epicenter. Solid lines represent theoretical travel-time curves predicted using the Earth model IASP91. In this distance range, the first arrivals are Pn phases. After removing high-noise traces, 22 seismograms were used in this study for seismogram stacking.

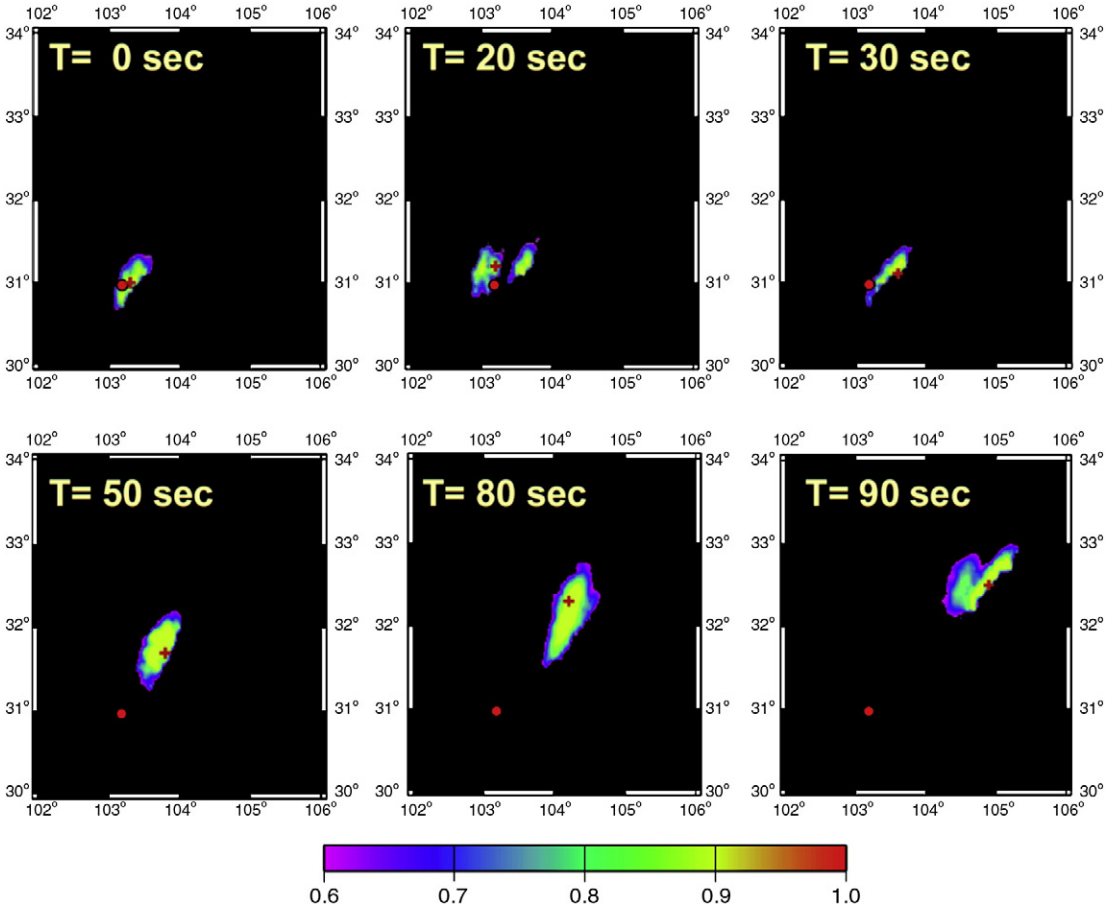

Fig. 7. Snapshots of back-projection imaging for rupture processes of the 2008 Wenchuan earthquake using BATS observations. Each panel shows the spatial distribution of radiated seismic energy from the fault plane at the stated time after initiation of the earthquake. The epicenter is indicated by the red solid circle. The red cross represents the peak value in the stacked image. The color area in each panel represents the region in which the radiated seismic energy is greater than 60% of the peak value. The color bar is shown in the bottom.

provides an independent estimate of the rupture duration of the 2008 Wenchuan earthquake, yielding a duration of approximately 100 s, and indicates that the rupture propagated northward along the Longmenshan Fault over a distance of more than 280 km from the initial rupture point.

We analyzed the VBSN array data using the same procedure as for the BATS array observations. The source area was configured using grid points, in the same manner as for the BATS data. The first arrivals in all VBSN array seismograms are Pn phases (Fig. 6). Data were band-pass filtered within 0.2 and 1.0 Hz. We then aligned all the seismograms and back-projected the first window seismic energy (i.e., the initial rupture) to the epicenter based on the computed travel times of the IASP91 model. Relative time shifts for each grid point and time steps were calculated for stacking. As for BATS, we processed source images for a duration of approximately 100 s.

Fig. 8 shows snapshots of seismic energy radiating from the fault plane at various times after the initial rupture. The images show the northward propagation of the source rupture; however, the imaged slip asperities from the VBSN array are larger than those from the BATS array (compare Figs. 7 and 8). Some artifacts are apparent near the northeastern end of the fault, as shown in the snapshot at 100 s (Fig. 8). The discrepancy between the results from the two arrays can be explained by the fact that source images were individually determined by each array using seismic energy radiating from a limited aperture, and that the two arrays have different azimuths to the source. Nevertheless, both arrays imaged the rupture propagating from the epicenter in the southwest to the northeast over a distance of approximately 280 km.

A joint estimation of the source rupture of the 2008 Wenchuan earthquake using observations from the two arrays may increase the aperture and reduce artifacts, thereby enabling imaging of the rupture processes and stabilized imaging results. We determined the source rupture processes by processing BATS and VBSN array data using Eq. (2) and the procedure described in the Methods section. In principle, the two arrays may make different contributions to the construction of source images. For example, BATS is located perpendicular to the strike of the ruptured fault plane and is sensitive to rupture propagation. In contrast, VBSN is located at shorter epicenter distances and has a larger azimuth gap compared with BATS. In the present study, we assumed the same weighting factor for both arrays.

Fig. 9 shows snapshots (at 10-second intervals) of seismic energy radiating from the fault plane following the initial rupture. The results obtained from joint imaging of the two arrays show the same rupture pattern as that obtained from the single arrays, but with significantly less artifact. In detail, Fig. 9 shows a stable moving source rupture from the epicenter, with variable rupture speed, to the northeastern end of the ruptured fault.

To understand the final slip distribution upon the fault plan, we processed a time-integrated stack that sums the radiated seismic energy for each grid point of the source plane during the rupture process. Fig. 10 shows the stacked seismic energy radiated from the fault plane, revealing a pattern similar to that of the final slip distribution on the fault plane. The bulk of the seismic energy is radiated from a major asperity located nearly 100 km from the epicenter, with a length of 70 km along the rupture fault. A comparison of our estimation with the results of a previous field investigation (Xu et al., 2008) reveals that this asperity is located on the Yingxiu–Beichuan Fault near Beichuan County. The snapshots of source rupture imaged in the present study indicate that the rupturing of this major asperity began at 50 s after the initial rupture (Fig. 11).

We reconstructed the time–distance relation of fault rupture slip related to the 2008 Wenchuan earthquake to show the propagation

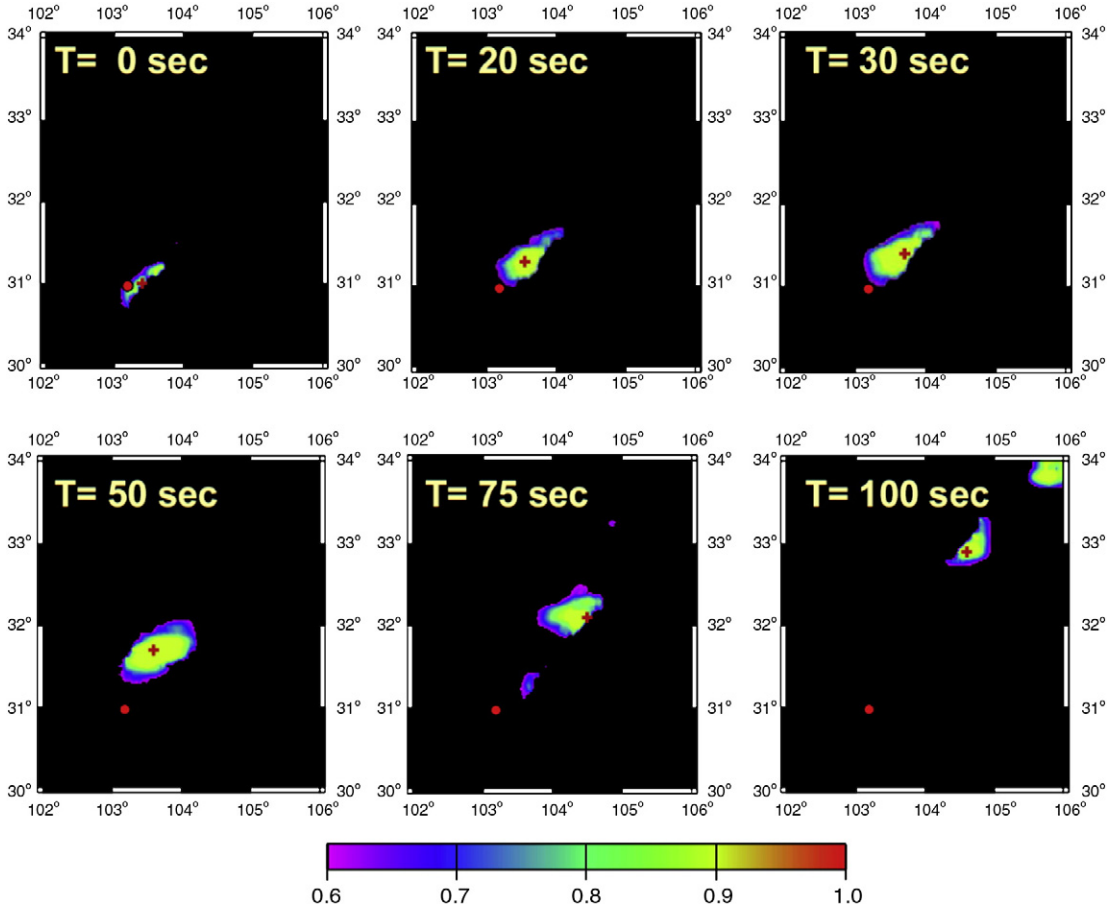

Fig. 8. As for Fig. 7, but using VBSN observations.

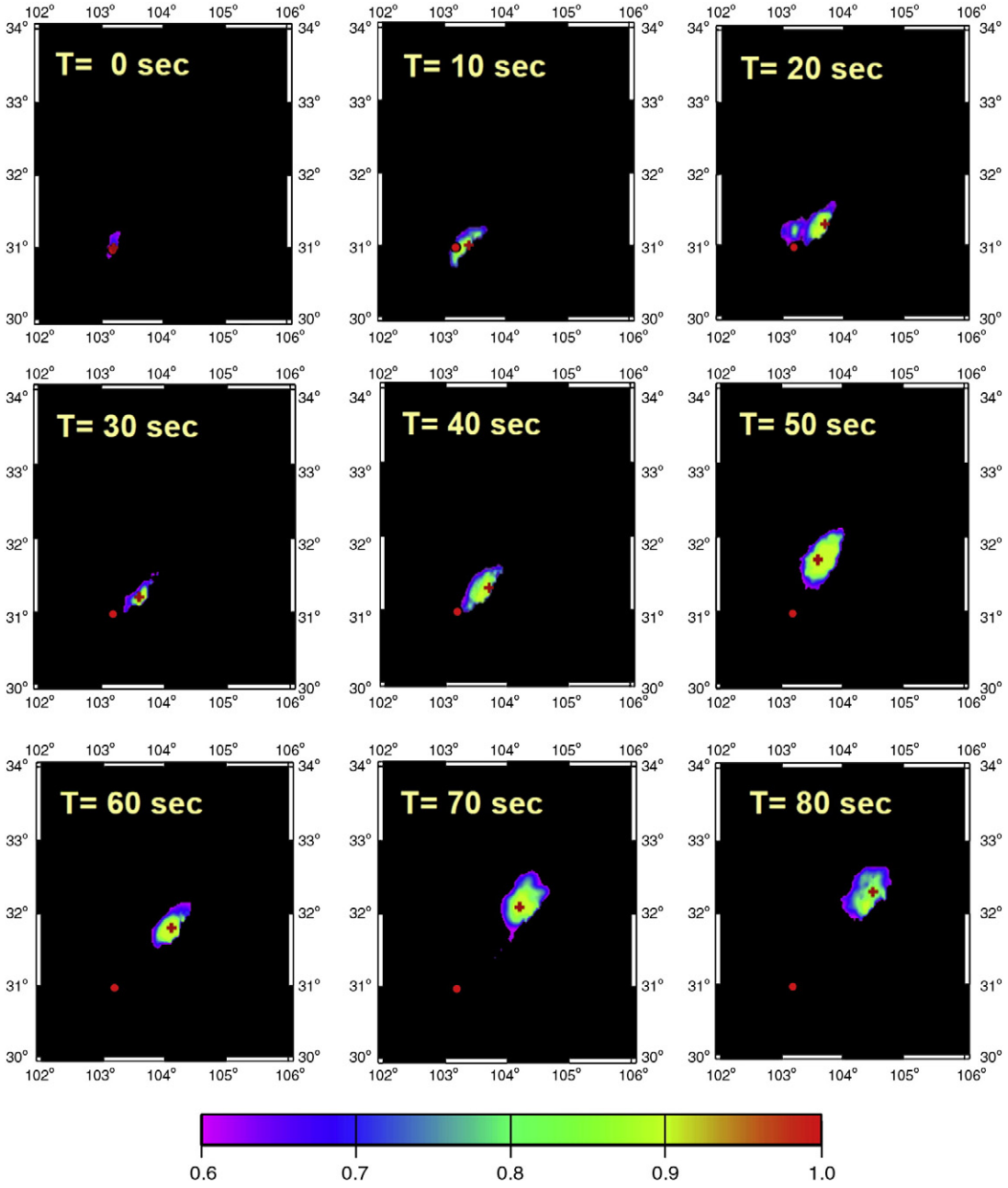

Fig. 9. As for Fig. 7, but using joint BATS and VBSN observations.

of the rupture (Fig. 12), based on the positions and times of the maximum stack amplitude for each time window of arrays (Figs. 7–9). The total rupture length was approximately 280 km and the duration time was nearly 100 s. Moreover, the results show that propagation of the fault rupture was mainly unilaterally northeastward with an average rupture speed of approximately 2.8 km/s, although the rupture speed was variable. The rupture began near the southwestern end of the earthquake fault with a rupture velocity of approximately 1.3 km/s; this slow rupture continued for about 30 s, when the rupture velocity increased to 3.1 km/s for a duration of about 50 s. Near the northeastern end of the fault, the fault rupture speed increased to 4.5 km/s before rupturing finally ceased (Fig. 12).

5. Discussion and conclusions

For source imaging, waveform inversions require an indirect procedure to fit observations using a set of theoretical Green's functions computed from an earth model. The inversion results depend on the accuracy of the theoretical earth model and the computed Green's functions. Various approaches have been proposed to avoid the use of an indirect waveform-inversion procedure, such as direct back-projection of the seismic energy of teleseismic body waves to the source rupture plane to obtain source imaging (Xu et al., 2009c). In other attempts to improve the spatial resolution of source imaging, the spare Global Seismographic Network data were replaced with dense seismic array observations at teleseismic distances, which provides high-frequency coherent array signals with which to perform high-resolution source imaging (Ishii et al., 2005; Krüger and Ohrnberger, 2005a). These approaches have been successfully applied to the 2008 Wenchuan earthquake (Du et al., 2009; Xu et al., 2009c).

Although the back-projection approach has been previously employed to study the source rupture, the success of this method is strongly dependent on the azimuth resolution of slips on the fault plane, as observed by a seismic array (Krüger and Ohrnberger,

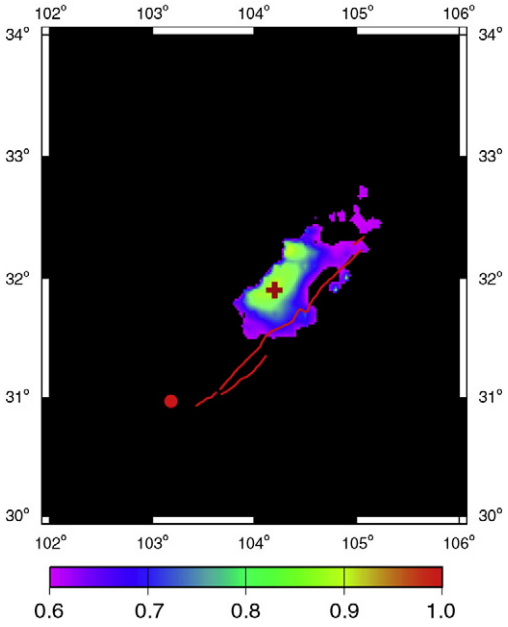

Fig. 10. Distribution of time-integrated seismic energy of the source region. The red lines show the surface segments of the earthquake rupture fault. Other symbols are that as for Fig. 7.

2005b). Thus, multiple seismic arrays from different azimuths should yield a higher resolution than a single array when imaging the source rupture. Furthermore, there are few cases in which this approach can be applied to imaging the source rupture at regional distances. For a finite fault, array observations from regional distances should have a larger azimuth resolution than those from arrays at teleseismic distances; however, a potential problem in this regard is the triplication of body wave arrivals from the upper mantle transition zone. The problem of multi-path body wave arrivals at regional distances can be overcome by using surface waves for source imaging (Valle´e et al., 2008); however, the uncertainty inherent in surface dispersion behavior must be carefully considered when estimating the rupture source.

Mori and Smyth (2009) are the only study to successfully image the source rupture of the Wenchuan earthquake using P-wave array data at regional distances. These authors employed the short-period vertical components of the Hi-Net array in Japan, operated by the National Institute for Earth Science and Disaster Prevention. The array is located at distances of 23°–35° from the Wenchuan earthquake and clearly recorded the direct P-wave of this event. Their resolved images provide the slip distribution at a higher spatial resolution than that possible from most teleseismic waveform inversions.

A similar approach was tested in the present study, using new array data from BATS and VBSN. In our analysis, the main features of the observations of the Wenchuan earthquake are that high-spatial-density broadband seismometers were used at a short distance to the epicenter, and the same as those observations for source rupture are approaching from two arrays at different azimuths. The use of arrays with a high station density enabled us to effectively use the relative differences in arrival time across each array to determine the approach azimuths of the incident seismic waves at a higher frequency. In addition, observations from a wide range of azimuths (based on two arrays) are useful for reducing artifacts in the source image.

Our analysis resolved a major asperity during the 2008 Wenchuan earthquake (Figs. 10 and 11). The results indicate that the largest slip occurred at more than 50 s after the initial rupture. In fact, the rupture process can be continuously traced in time for nearly 100 s, with an average rupture speed of 2.8 km/s, which is comparable with estimates of the source rupture process made using data from teleseismic and regional distances based on body waveform inversion or array stacking (Du et al., 2009; Mori and Smyth, 2009; Wang et al., 2008; Xu et al., 2009c; Zhang and Ge, 2010). However, the estimated rupture slip details vary among these studies.

By analyzing a simple fault plane, we detected a single large asperity and rupture propagation at varying speeds during the rupture process (Fig. 12). Wang et al. (2008) proposed a variably dipping and discontinuous fault plane related to the 2008 Wenchuan earthquake. The authors inverted two major asperities, located at Yingxiu and Beichuan, with an average rupture speed of 2.7 km/s. Du et al. (2009) resolved two segment ruptures: one with a length of 110 km, an average rupture speed of 2.2 km/s, and a duration about 50 s; and a second segment that continued the rupture with a duration of about 40 s, length of 190 km, and a rupture speed of 4.8 km/s. Xu et al. (2009c) determined three distinct pulses, with the largest asperity occurring at 23 s after the origin time; the average rupture speed was 2.8 km/s. Mori and Smyth (2009) detected a large asperity that was ruptured 60 s after the origin time, and estimated an average rupture speed of approximately 3.0 km/s. Finally, Zhang and Ge (2010) reported a double-asperity rupture process with a mean rupture speed of about 3.0 km/s.

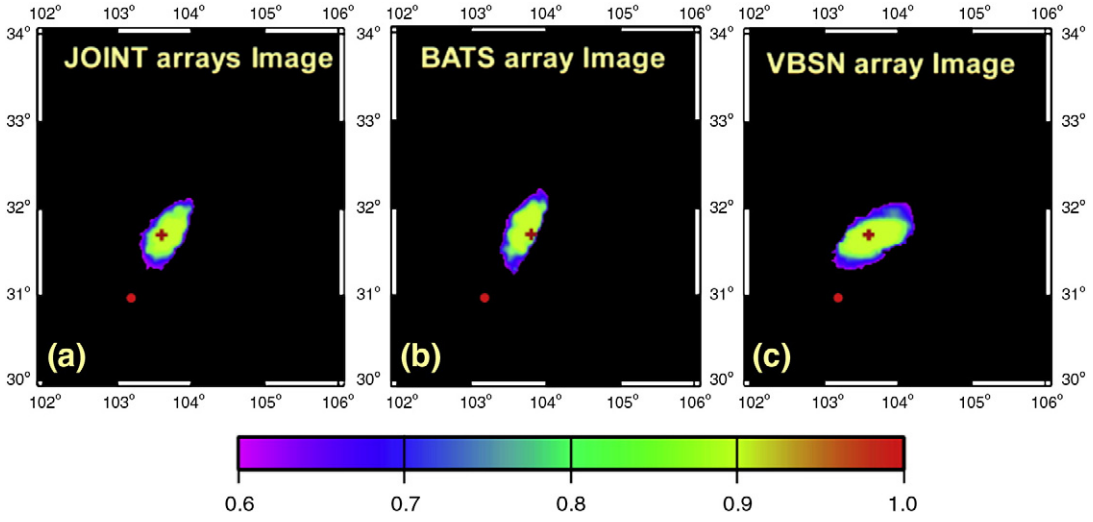

Fig. 11. (a) Snapshot of back-projection imaging from joint BATS and VBSN observations at 50 s after the earthquake occurrence. (b). Snapshot at 50 s using BATS data. (c). Snapshot at 50 s using VBSN data.

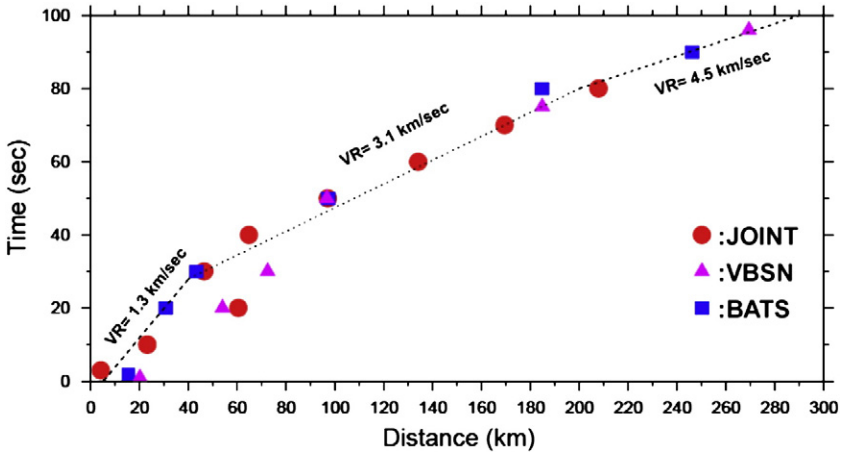

Fig. 12. Relation between rupture distance and time during the entire source rupture of the 2008 Wenchuan earthquake. Data were estimated using snapshots from Fig. 7 for BATS (blue squares), from Fig. 8 for VBSN (purple triangles), and from Fig. 9 for JOINT (red solid circles representing the sum of the two arrays). The rupture distance was estimated from the epicenter to the location of the peak amplitude of each snapshot. Dashed lines represent the distance–time relation for the three stages of the rupture process. The average rupture velocity of this earthquake was approximately 2.8 km/s.

The above estimates of the source rupture were based on seismic data recorded far from the epicenter (i.e., at regional or teleseismic distances), recorded with a range of different sensors; consequently, the discrepancies in rupture velocities and asperity sizes may reflect the individual characteristics of the seismic data. In addition, these studies were based on several simplification assumptions. To interpret and verify the rupture behavior in detail, it is necessary to assess the validity of these assumptions or to correct them in the future. Furthermore, new data from multiple near-source strong motion observations (Li et al., 2008) would be useful in resolving the discrepancies among studies.

As shown in the present study, the application of back-projection mapping requires no prior knowledge of the fault geometry, fault dimensions, or rupture duration to image the source rupture process. Only the first-arrival P-wave trains are used in the imaging process. Furthermore, in the present study, the fault planes are simplified as planar surface projected downward from the surface to the depth of epicenter. The results of our previous tests (Huang et al. 2011) show that the determined source images suffer from minor distortion when using this planar-projected fault plane. Accordingly, this approach could be implemented in a real-time system to estimate the length of fault rupture and the duration of great earthquakes using limited source information. This procedure may be faster than the inversion approach using global network waveforms because it enables us to rapidly identify, evaluate, and report disasters arising from great earthquakes at remote sites. For example, this approach could have been applied to the 2005 Kashmir earthquake (Owen et al., 2008; USGS, 2006) and the 2004 Sumatra–Andaman earthquake to rapidly provide information on the source rupture properties, thereby helping to evaluate damage arising from massive landslides and tsunami, which is important for subsequent relief efforts.

In summary, we successfully imaged the source rupture processes of the 2008 Wenchuan earthquake from two regional seismic array observations using a back-projection method. The results indicate that this event had a rupture duration of nearly 100 s, with major asperities radiating energy at 50 s after the initiation of earthquake rupture. The fault rupture initiated at its epicenter and extended unilaterally to the northeast for about 280 km. Although the average rupture velocity was estimated to be approximately 2.8 km/s, the entire source rupture comprised three segments with different rupture speeds. The rupture began near the southwestern end of the earthquake fault with a rupture velocity of approximately 1.3 km/s; this slow rupture continued for about 30 s, after which time the rupture velocity increased to 3.1 km/s for a duration of about 50 s. Near the northeastern end of the fault, the fault rupture speed increased to 4.5 km/s before rupturing ceased.

Acknowledgements

The authors thank the Institute of Geophysics, Vietnamese Academy of Science and Technology, the Central Weather Bureau, and the Institute of Earth Sciences, Academia Sinica, for assisting field works and providing the data used in this study. We also thank Dr. Li Zhao, Dr. C. F. Chen, Prof. X. F. Chen, and Prof. L. P. Zhu for their useful comments and valuable discussions. GMT (Wessel and Smith, 1995) was used to create some of the figures. This study was supported by Academia Sinica, the National Science Council, Taiwan (grant numbers 99-2116-M-001-022, 99-2116-M-001-002, and 99-2116-M-002-005), the National Natural Science Foundation of China (grant no. 40821160550) and State Key Laboratory of Earthquake Dynamics (grant no. LED-2008-A04).

References

Burchfiel, B.C., Royden, L.H., van der Hilst, R.D., Hager, B.H., Chen, Z., King, R.W., Li, C., Lü, J., Yao, H., Kirby, E., 2008. A geological and geophysical context for the Wenchuan earthquake of 12 May 2008, Sichuan, People's Republic of China. GSA Today 18 (7), 4–11. doi:10.1130/GSATG18A.1.

Chen, J.H., Liu, Q.Y., Li, S.C., Guo, B., Li, Y., Wang, J., Qi, S.H., 2009. Seismotectonic study by relocation of the Wenchuan Ms 8.0 earthquake sequence. Chinese Journal of Geophysics 52 (2), 390–397 (In Chinese with an English abstract).

Dong, S., Zhang, Y., Wu, Z., Yang, N., Ma, Y., Shi, W., Chen, Z., Long, C., Meijian, A.N., 2008. Surface rupture and co-seismic displacement produced by the Ms 8.0 Wenchuan earthquake of May 12th, 2008, Sihuan, China: Eastwards growth of the Qinghai-Tibet plateau. Acta Geologica Sinica 82, 938–948.

Du, H.L., Xu, L.S., Chen, Y.T., 2009. Rupture process of the 2008 great Webchuan earthquake from the analysis of the Alaska-array data, China. Chinese Journal of Geophysics 52, 372–378 (In Chinese with an English abstract).

ERI, 2008. Earthquake Research Institute, Univ. of Tokyo. http://www.eri.u-tokyo.ac.jp/topics/china2008/source_eng.html.

Huang, B.S., 2001. Evidence for azimuthal and temporal variations of the rupture propagation of the 1999 Chi-Chi, Taiwan earthquake from dense seismic array observations. Geophysical Research Letters 28, 3377–3380.

Huang, B.S., 2008. Tracking the North Korean nuclear explosion of 2006, using seismic data from Japan and satellite data from Taiwan. Physics of the Earth and Planetary Interiors 167, 34–38. doi:10.1016/j.pepi.2008.02.004.

Huang, Y.L., Huang, B.S., Wang, C., Wen, K., 2004. Numerical modeling for earthquake source imaging; implications for array design in determining the rupture process. TAO 15, 133–150.

Huang, B.S., Huang, Y.L., Lee, S.J., Chen, Y.G., Jiang, J.S., 2008a. Initial rupture processes of the 2006 Pingtung Earthquake from near source strong-motion records. TAO 19, 547–554.

Huang, Y., Wu, J.P., Zhang, T.Z., Zhang, D.N., 2008b. Relocation of the M8.0 Wenchuan earthquake and its aftershock sequence. Science in China, Series D: Earth Sciences 51 (12), 1703–1711. doi:10.1007/s11430-008-0135-z.

Huang, B.S., Le, T.S., Liu, C.C., Toan, D.V., Huang, W.G., Wu, Y.M., Chen, Y.G., Chang, W.Y., 2009. Portable broadband seismic network in Vietnam for investigating tectonic deformation, the Earth's Interior, and early-warning systems for earthquakes and tsunamis. Journal of Asian Earth Sciences 36, 110–118. doi:10.1016/j.jseaes.2009.02.012.

Huang, B.S., Huang, Y.L., Leu, P.L., Lee, S.J., 2011. Estimation of the rupture velocity and fault length of the 2004 Sumatra–Andaman earthquake using a dense broadband seismic array in Taiwan. Journal of Asian Earth Sciences 40, 762–769. doi:10.1016/j.jseaes.2010.10.020.

Ishii, M., Shearer, P., Houston, H., Vidale, J.E., 2005. Extent, duration and speed of the 2004 Sumatra-Andaman earthquake imaged by the Hi-Net array. Nature 435, 933–936.

Ishii, M., Shearer, P.M., Houston, H., Vidale, J.E., 2007. Teleseismic P wave imaging of the 26 December 2004 Sumatra-Andaman and 28 March 2005 Sumatra earthquake ruptures using the Hi-net array. Journal of Geophysical Research 112, B11307. doi:10.1029/2006JB004700.

Ji, C., 2008. Preliminary result of the May 12, 2008 Mw 7.97 ShiChuan earthquake. http://www.geol.ucsb.edu/faculty/ji/big_earthquakes/2008/05/12/ShiChuan.html.

Kao, H., Jian, P.R., Ma, K.F., Huang, B.S., Liu, C.C., 1998. Moment-tensor inversion for offshore earthquakes east of Taiwan and their implications to regional collision. Geophysical Research Letters 25, 3619–3622.

Kennett, B.L.N., Engdahl, E.R., 1991. Traveltimes for global earthquake location and phase identification. Geophysical Journal International 105, 429–465.

Krüger, F., Ohrnberger, M., 2005a. Spatio-temporal source characteristics of the 26 December 2004 Sumatra earthquake as imaged by teleseismic broadband arrays. Geophysical Research Letters 32 (24), L24312. doi:10.1029/2005GL023939.

Krüger, F., Ohrnberger, M., 2005b. Tracking the rupture of the $M_w = 9.3$ Sumatra earthquake over 1,150 km at teleseismic distance. Nature 435, 937–939. doi:10.1038/nature03696.

Li, X., Zhou, Z., Huang, M., Wen, R., Yu, H., Lu, D., Zhou, Y., Cui, J., 2008. Preliminary analysis of strong-motion recordings from the magnitude 8.0 Wenchuan, China earthquake of May 12, 2008. Seismological Research Letters 79, 844–854.

Mori, J., Smyth, C., 2009. A Summary of Seismological Observations for the May 12, 2008 Wenchuan, China earthquake, in *Investigation report of the 2008 Wenchuan Earthquake, China, Grant-in-Aid for Special Purposes of 2008, MEXT, No. 2090002*. http:/shake.iis.u-tokyo.ac.jp/wenchuan/index.html.

Nagoya, 2008. Research Center for Seismology, Volcanology and Disaster Mitigation, Nagoya Univ. http://www.seis.nagoya-u.ac.jp/sanchu/Seismo_Note/2008/NGY8a.html.

Nishimura, N., Yagi, Y., 2008. Rupture process for May 12, 2008 Sichuan earthquake (preliminary result). http://www.geol.tsukuba.ac.jp/~nisimura/20080512/.

Owen, L.A., Kamp, U., Khattak, G.A., Harp, E.L., Keefer, D.K., Bauer, M.A., 2008. Landslides triggered by the 8 October 2005 Kashmir earthquake. Geomorphology 94 (1–2), 1–9.

Rost, S., Thomas, C., 2002. Array seismology, methods and applications. Reviews of Geophysics 40, 2-1–2-27.

Shen, Z.-K., Sun, J., Zhang, P.Z., Wan, Y., Wang, M., Bürgmann, R., Zeng, Y., Gan, W., Liao, H., Wang, Q., 2009. Slip maxima at fault junctions and rupturing of barriers during the 2008 Wenchuan earthquake. Nature Geoscience 2, 718–724. doi:10.1038/NGEO1636.

USGS, 2006. U.S. Geological Survey, Magnitude 7.6 – Pakistan earthquake – usdyae, 2005 October 8, 03:50:38 UTC (2006). http://earthquake.usgs.gov/eqcenter/eqinthenews/2005.

Valle´e, M., Lande`s, M., Shapiro, N.M., Klinger, Y., 2008. The 14 November 2001 Kokoxili (Tibet) earthquake: High-frequency seismic radiation originating from the transitions between sub-Rayleigh and supershear rupture velocity regimes. Journal of Geophysical Research 113, B07305. doi:10.1029/2007JB005520.

Walck, M.C., 1984. The P-wave upper mantle structure beneath an active spreading center: the Gulf of California. Geophysical Journal of the Royal Astronomical Society 76, 697–723.

Wang, W., Zhao, L., Li, J., Yao, Zh., 2008. Rupture process of the Ms 8.0 Wenchuan earthquake of Sichuan, China. Chinese Journal of Geophysics 51, 1403–1410 (In Chinese with an English abstract).

Wessel, P., Smith, W.H.F., 1995. A new version of the Generic Mapping Tools (GMT), Eos Trans. AGU 76, 329.

Xu, X.W., Wen, X.Z., Ye, J.Q., Ma, B.Q., Chen, J., Zhou, R.J., He, H.L., Tian, Q.J., He, Y.L., Wang, Z.C., Sun, Z.M., Feng, X.J., Yu, G.H., Chen, L.C., Chen, G.H., Yu, S.E., Ran, Y.K., Li, X.G., Li, C.X., An, Y.F., 2008. The Ms 8.0 Wenchuan earthquake surface ruptures and its seismogenic structure. Seismology and Geology 30 (3), 597–629 (in Chinese).

Xu, X., Yu, G., Chen, G., Ran, Y., Li, C., Chen, Y., Chang, C., 2009a. Parameters of coseismic reverse- and oblique-slip surface ruptures of the 2008 Wenchuan Earthquake, Eastern Tibetan Plateau. Acat Geologia Sinica 83, 673–684. doi:10.1111/j.1755-6724.2009.00091.x.

Xu, X., Wen, X., Yu, G., Chen, G., Klinger, Y., Hubbard, J., Shaw, J., 2009b. Coseismic reverse- and oblique-slip surface faulting generated by the 2008 Mw 7.9Wenchuan earthquake, China. Geology 37, 515–518.

Xu, Y., Koper, K.D., Sufri, O., Zhu, L., Hutko, A.R., 2009c. Rupture imaging of theM_w7.9 12 May 2008 Wenchuan earthquake from back projection of teleseismic*P*waves. Geochemistry, Geophysics, Geosystems 10, Q04006. doi:10.1029/2008GC002335.

Zhang, H., Ge, Z.X., 2010. Tracking the Rupture of the 2008 Wenchuan Earthquake by Using the Relative Back-Projection Method. Bulletin of the Seismological Society of America 100, 2551–2560. doi:10.1785/0120090243.

Zhang, P.Z., Xu, X.W., Wen, X.Z., Ran, Y.K., 2008. Slip rates and recurrence intervals of the Longmen Shan active fault zone and tectonic implications for the mechanism of the May 12 Wenchuan earthquake, 2008, Sichuan, China. Chinese Journal of Geophysics 51 (4), 66–107.

Zhang, P.Z., Wen, X.Z., Shen, Z.K., Chen, J.H., 2010. Oblique, High-Angle, Listric-Reverse Faulting and Associated Development of Strain: The Wenchuan Earthquake of May 12, 2008, Sichuan, China. Annual Review of Earth and Planetary Sciences 38, 353–382. doi:10.1146/annurev-earth-040809-152602.